Available online at www.sciencedirect.com

SciVerse ScienceDirect

Procedia Engineering 38 (2012) 1524 – 1530

Procedia Engineering

www.elsevier.com/locate/procedia

International Conference on Modelling, Optimisation and Computing (ICMOC 2012), April 10 - 11, 2012

CFD simulation to optimise single stage pulse tube refrigerator temperature below 6oK

S.K. Rout[a*], R. Mukare[a], B.K. Choudhury[a], R.K. Sahoo[a], S.K. Sarangi[a]

[a] *Department of Mechanical Engineering, NIT Rourkela-769008, Odisha, India.*

Abstract

An optimize result of the single stage iterance tube pulse tube refrigerator (ITPTR) has been found by the use of a computational fluid dynamic (CFD) solution method. A well CFD solution software FLUENT is used for solution purpose. A number of case has been solved by changing the pulse tube length by taking diameter constant out of which it is found that a length of about 125mm at which the minimum temperature is achieved at cold heat exchanger end of 58 K. The variation in any parameter of ITPTR will affect the cooling temperature that may be the length or diameter of pulse tube or inertance tube or change in operating frequency but it is essential to achieve lower temperature than till date achieved by same method. So for optimization purpose we take the length of pulse tube length as the varying Parameter and the operating frequency 34 Hz, pulse tube diameter 5mm remains constant. To get an optimum parameter experimentally is a very tedious for iterance tube pulse tube refrigerator job so the CFD approach gives a better solution which is the main purpose of the present work.

Keywords: Pulse tube; regenerator; porous zone; CFD; Heat Exchanger

* Corresponding author. Tel.: +91-889-5815648.
Email: sachindranit@gmail.com

1. Introduction

Due to no moving part and high reliability pulse tube refrigerator are widely used for space cooling applications, semiconductor fabrication for industrial purpose, infrared sensors in military field etc. In

1877-7058 © 2012 Published by Elsevier Ltd. Open access under CC BY-NC-ND license.
doi:10.1016/j.proeng.2012.06.188

world history Gifford and Logesworth [1] first time give the idea of Basic pulse tube Refrigerator (BPTR) in 1960s. After 16 year later Mikuluin [2] bring a modification to the introductory type Basic pulse tube Refrigerator. To get better cooling effect he modified it in such a way that the phase angle between temperature and velocity changes due to adding a small orifice which causes enthalpy flow increasing near hot end. Such type of pulse type of refrigerator is named as Orifice Pulse Tube Refrigerator (OPTR). Then it is modified by so many researchers to get better cooling effect by varying shape of any parameter or number of stage. A double inlet pulse tube refrigerator (DIPTR) has been introduced by Zhu et al. [3]. Marquardt and Redebaugh [4] made another type of refrigerator having much better efficiency by combining both iterance tube and orifice. There are some other papers which deal with theoretical approaches to study the phase shift, efficiency and flow cycles [5-10] inside the pulse tube refrigerator. Cha et al. [11] first time made a CFD model on a single stage iterance pulse tube refrigerator using FLUENT software which gives a better solution to optimise pulse tube refrigerator. Using the same CFD

Nomenclature

a	piston displacement (m)
a_0	piston displacement amplitude (m)
C_p	specific gas constant, (J/kg-K)
C	inertial resistance (m^{-1})
E	total energy (JKg^{-1})
h	enthalpy (J/kg)
j	superficial velocity (m/s)
k	thermal conductivity (W/m-K)
p	pressure (N/m^2)
T	temperature (K)
t	time (s)
v	velocity (m/s)
V	volume (m^3)
S_x,S_y	momentum source terms (Nm^{-3})

Greek Symbols

ρ	density (kg/m^3)
ω	angular frequency (rad/s)
ψ	permeability tensors (m^2)
μ	dynamic viscosity(kg/m s)
ν	kinematic viscosity
τ	stress tensors (N/m^2)
ξ	porosity

Subscripts

S	solid
f	fluid
z	frequency
y	radial coordinate
x	axial coordinate

solution method by changing the dimension of (ITPTR). Ashwin et al. [12] achieved a minimum temperature of 65 K at an operating frequency of 34 Hz. Ling et al. [13] studied the thermodynamic cycles inside a pulse tube refrigerator. They show a minimum temperature achieved is of 62k, operating at a higher frequency of 40Hz.

2. Geometrical Design of PTR for CFD analysis

2.1. Mathematical Formulation

Fig. 1 shows the schematic representation of the 2D axi-symmetric model of the inertance pulse tube refrigerator used for the present computational analysis. The detail dimension is given in the Table 1. at which the optimised temperature was found.

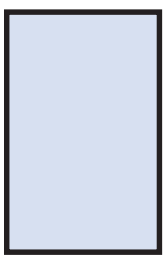

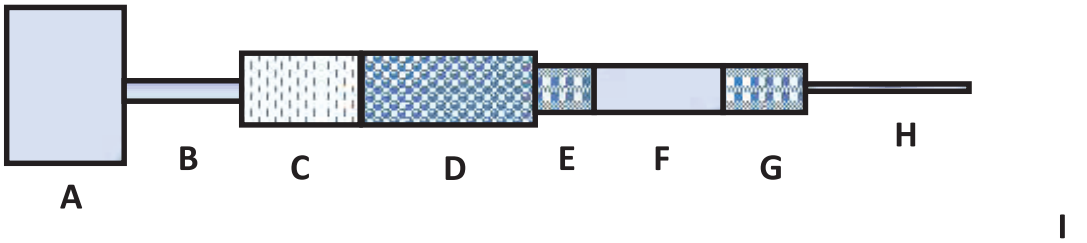

Fig. 1. Schematic diagram of computational domain of ITPTR: A - compressor, B – transfer line, C - after cooler, D – regenerator, E – cold heat exchanger, F – pulse tube, G – hot heat exchanger, H - inertance tube, I - reservoir.

Table1

constituent part	*Diameter (m)*	*Length (m)*	*Boundary condition*
Compressor (A)	0.01908	0.0075	Adiabatic
Transfer line (B)	0.0031	0.101	Adiabatic
After cooler (C)	0.008	0.02	300 K
Regenerator (D)	0.008	0.058	Adiabatic
Cold heat exchanger (E)	0.006	0.0057	Adiabatic
Pulse tube (F)	0.005	0.125	Adiabatic
Hot heat exchanger(G)	0.008	0.01	300 K
Inertance tube (H)	0.00085	0.684	Adiabatic
Reservoir (I)	0.026	0.13	Adiabatic

2.2. Governing equations

The governing equations for the above analysis can be written as:

Continuity Equation

$$\frac{\partial}{\partial t}\left[\xi\rho\right]+\frac{1}{y}\frac{\partial}{\partial y}\left[\xi r\rho_y\right]+\frac{\partial}{\partial x}\left[\xi\rho_f v_x\right]=0 \quad (1)$$

Momentum Equation:

For axial direction

$$\frac{\partial}{\partial t}\left[\xi\rho v_x\right]+\frac{1}{y}\frac{\partial}{\partial x}\left[\xi r v_x\right]v_x+\frac{1}{y}\left[\frac{\partial}{\partial y}\left[\xi y\ \rho_f v\right]v_y\right]=\frac{\xi p}{}\frac{\partial}{\partial y}+$$
$$\frac{1}{y}\frac{\partial}{\partial y}\left\{y\mu\left(2\frac{\xi v_x}{\partial x}-\frac{2}{3}\left(\nabla\ \xi\right).v\right)\right\}+\frac{1}{}\left[\frac{1}{y}\frac{\partial}{\partial y}\left[y\mu\left\{\frac{\xi v_x\xi\partial v_y}{\partial y}\right\}\right]\right]\frac{x}{y} \quad (2)$$

For radial direction

$$\frac{\partial}{\partial t}\left[\xi\rho_f v_y\right]+\frac{1}{y}\frac{\partial}{\partial x}\left[\xi r v_x v_y\right]+\frac{1}{y}\frac{\partial}{\partial y}\left[y\xi\rho_f v_y v_y\right]=-\frac{\partial p}{\partial y}+$$
$$\frac{1}{r}\frac{\partial}{\partial x}\left\{2x\mu\left(\frac{\partial v_x}{\partial x}-\frac{1}{3}\left(\vec{\nabla}.\vec{v}\right)\right)\right\}+\frac{1}{y}\frac{\partial}{\partial y}\left\{2y\mu\left[\frac{\partial v_x}{\partial y}-\frac{1}{3}\left(\vec{\nabla}.\vec{v}\right)\right]\right\} \quad (3)$$
$$+\frac{2\mu}{y}\left[\frac{\left(\vec{\nabla}.\vec{v}\right)}{3}-\frac{v_y}{y}\left(\vec{\nabla}.\vec{v}\right)\right]+S_y$$

Where S_x and S_y are the two source term in the axial and radial direction which values is zero for nonporous zone. But for the porous zone the source term which is solved by the solver is given by the following equation.

$$S_x=-\left(\frac{\mu}{\psi}v_x+\frac{1}{2}C\rho_f\left|v\right|v_x\right) \quad (4)$$

$$S_y=-\left(\frac{\mu}{\psi}v_y+\frac{1}{2}C\rho_f\left|v\right|v_y\right) \quad (5)$$

In the above equation the first term is called Darcy term and the second term is called the Forchheimer term which are responsible for the pressure drop inside the porous zone.

Energy Equation:

$$\frac{\partial}{\partial t}\left(\xi\rho E_f+\left(1-\xi\right)\rho_s E_s\right)+\vec{\nabla}.\left(\vec{v}\left(\rho_f E_f+p\right)\right)=\vec{\nabla}.\left(k\vec{\nabla}T_f+\tau.\vec{v}\right) \quad (6)$$

Where

$$k=\xi k_f+\left(1-\xi\right)k_s \quad (7)$$

$$E_f=h-p/\rho_f+v^2/2 \quad (8)$$

2.3. Detail modeling and Boundary Conditions

All the boundary condition with dimension is shown in Table 1. Similar type of 2-D Axi-symmetric geometry was modelled using the modelling software GAMBIT as shown in Fig. 1. The number of mesh for this case is 4400 which is chosen after a grid independency test which shows that after this value there no variation in the result of simulation. To guide the compressor piston a FLUENT User Define Function (UDF) is attached to the piston with a correlation $a = a_{0*} \sin*(\omega t)$. The operating frequency is taken z = 34 Hz. Where a is the piston displacement and a_0 = 0.0045m is the amplitude with a time increment of 0.0007s is assumed and the piston head velocity is related with the correlation $v = a_{0*}\omega*\cos*(\omega t)$. Where v is the piston head velocity. For porous media region the parameter s are taken from [15], inertial resistance 76090 m^{-1} and permeability 1.06×10^{-10} m^2. Steel is chosen as the component material. The working gas is chosen is helium and the property (viscosity, thermal conductivity, specific heat) of the gas are taken as temperature dependent from NIST data base.

2.4. Numerical solution procedure

The governing equations as described above are solved by Fluent. Axisymmetric, unsteady, cell based, physical velocity with segregated solver is taken for analysis. PISO algorithm with a PRESTO (Pressure Staggered Option) scheme for the pressure velocity coupling is used for the pressure correction equation. Suitable Under relaxation factors for pressure, momentum and for energy were used for the better convergence. Quad lateral cells were used for the entire computational domain. For all equation Convergence of the discretized equations are said to have been achieved when the whole field residual was kept at 10^{-6}.

3. Results and discussion

3.1. Matching with Cha et al. [11] model

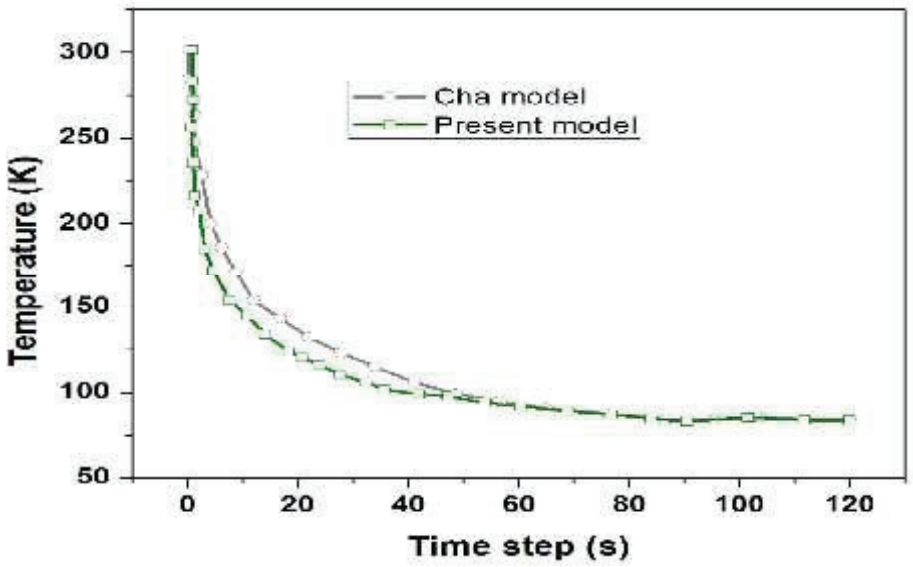

Fig. 2. Validation plot between present model and Cha et al. [11] model

The Fig. 2 shows that the present CFD results match well with the Cha et al. [11] model. It is noticeable from the Fig. 3 that the steady state temperature is reached after 50s for both the case after which there no change in temperature with respect to time. The Cha et al. model reporting a temperature of 87 K using 4200 number of cell where in the present case it is found a 86 K using 3900 cell.

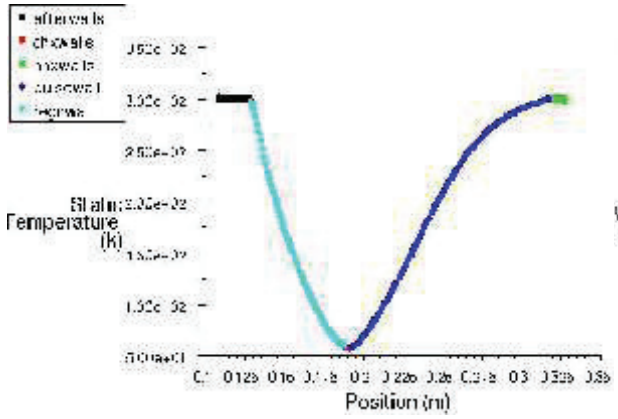

Fig. 3.

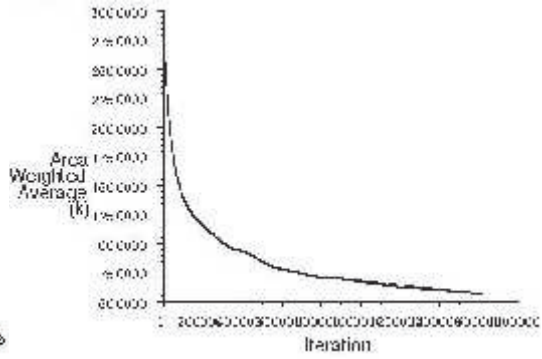

Fig. 4.

Fig. 3. Axial temperature plot varying from after cooler to hot heat exchanger after steady state temperature of 58k at cold heat exchanger .

Fig. 4. Area weighted verage temperature plot with number of iteration step.

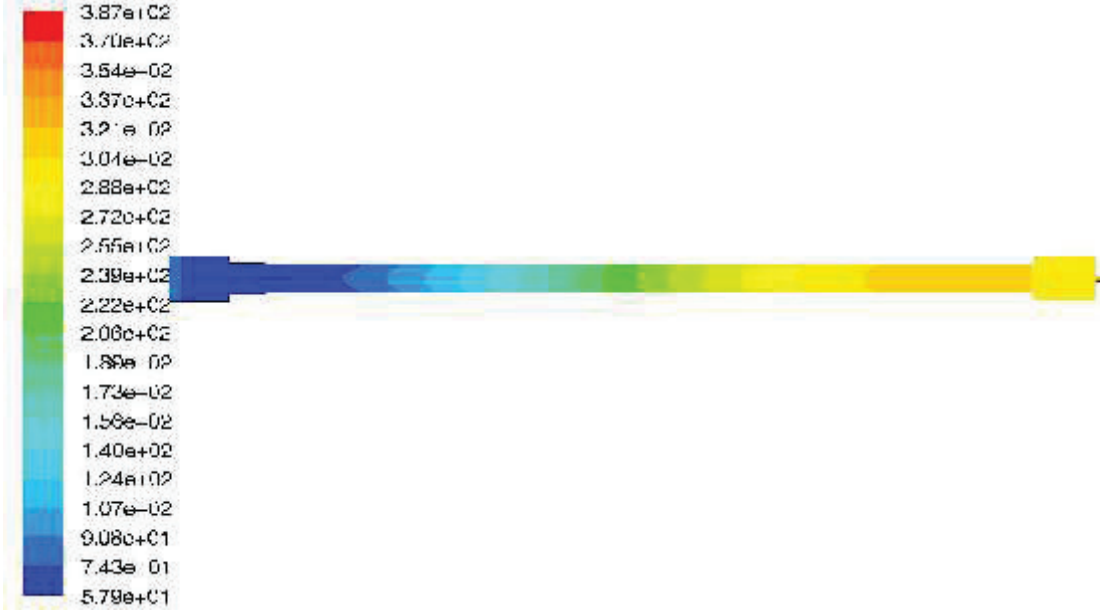

Fig. 5. Temperature Contours showing the temperature variation inside pulse tube.

3.2. Discussion on cool down Temperature

Fig. 3 shows the axial temperature variation from after cooler wall to hot heat exchanger wall because this is the region at which it gives the minimum temperature. The plot is taken after a steady state is achieved. So at any time the temperature remains nearly constant with small fluctuation at any position. Near the cold heat exchanger wall it is found that 58 K where after cooler wall and hot heat exchanger wall is at 300k. Fig. 4 shows the area weighted average temperature at cold heat exchanger with respect to number of iteration till 800000 steps. It shows that initially temperature decreases firstly and gradually the rate of decrease in temperature decreases and becomes steady. Fig. 5 shows the Contours how the temperature varies inside pulse tube.

4. Conclusions

The study focuses on CFD investigation to optimise the pulse tube refrigerator dimension so that we get a better cooling effect to generate liquid nitrogen which requires a temperature below 77 K. The present investigation shows as per requirement result for producing liquid nitrogen using Pulse tube refrigerator. This cooling temperature is achieved numerically by changing the dimension of pulse tube length to 125mm. With this dimension we get the temperature 58K at cold heat exchanger.

References

[1] Gifford W, Longsworth R .Pulse-tube refrigeration .*Trans ASME, J Eng Ind* (series B) 1964, 86:264–8
[2] Mikulin E, Tarasov A, Shrebyonock M .Low-temperature expansion pulse tubes, *Advances in Cryogenics Engineering* 1984, 29:629-637.
[3] Zhu S, Peiyi W, Zhonggi, Matsubara Y.Double inlet pulse tube refrigerator: an important improvement, *Cryogenics* 1990, 30: 514–520.
[4] E.D. Marquardt, R. Radebaugh .Pulse tube oxygen liquefier, *Advances in Cryogenics Engineering* 2000, 45: 457–464.
[5] de Boer, P C T .Thermodynamic analysis of the basic pulse-tube refrigerator, *Cryogenics* 1994, 34: 699-711
[6] Kittel P .Ideal orifice pulse tube refrigerator performance. *Cryogenics* 1992, 32: 843-844.
[7] Zhu, SW and Chen Z Q .Isothermal model of pulse tube refrigerator. *Cryogenics*1994, 34:591-595.
[8] Huang BJ and Chuang MD .System design of orifice pulse-tube refrigerator using linear flow network analysis. *Cryogenics*, 1996, 36:889-902.
[9] Kuriyama and Radebaugh R., Analysis of mass and energy flow rates in an orifice pulse-tube refrigerator .Cryogenics, 1999, 39: 85-92.
[10] Hoffmann A. and Pan H .Phase shifting in pulse tube refrigerators. *Cryogenics* 1999, 39:529-537.
[11] Cha JS, Ghiaasiaan SM .Multi-dimensional flow effects in pulse tube refrigerators. *Cryogenics* 2006, 46:658-665.
[12] Ashwin TR, Narasimham GSVL, Jacob S .CFD analysis of high frequency miniature pulse tube refrigerators for space applications with thermal non-equilibrium model. Cryogenics 2010, 30:152-166.
[13] Chen L, Zhang Y, Luo E, Li T, Wei X .CFD analysis of thermodynamic cycles in a pulse tube refrigerator, Cryogenics 2010, 50:743-749.
[14] Fluent 6.3 User's Guide, Fluent Inc., http://www.fluentusers.com.